Crystal Structure of the Ferredoxin I from *Desulfovibrio africanus* at 2.3 Å Resolution‡

Anne Séry,§ Dominique Housset,§ Laurence Serre,|| Jacques Bonicel,⊥ Claude Hatchikian,⊥ Michel Frey,*,§ and Michel Roth§

Laboratoire de Cristallographie et de Cristallogénèse des Protéines, Institut de Biologie Structurale J.-P. Ebel, CEA-CNRS, 41 avenue de Martyrs, 38027 Grenoble Cedex 1, France, and Unité de Bioénergétique et Ingéniérie des Protéines, 31 Chemin Joseph Aiguier, 13402 Marseille Cedex 20, France

Received July 13, 1994; Revised Manuscript Received October 3, 1994⊗

ABSTRACT: The crystal structure of the ferredoxin I from the sulfate-reducing bacterium *Desulfovibrio africanus* (DaFdI) has been solved and refined by X-ray diffraction. The crystals are orthorhombic with $a = 96.6$ Å, $b = 58.1$ Å, and $c = 20.7$ Å, space group $P2_12_12$, and two ferredoxin molecules per asymmetric unit. The initial electron density map has been obtained by combining phasing by molecular replacement methods, anomalous scattering, and noncrystallographic averaging. The final crystallographic R factor is 0.182 with 10−2.3 Å resolution data. In parallel, the amino acid sequence was redetermined. This showed that DaFdI contains 64 residues (instead of 61) including one free cysteine, one histidine, and one tryptophan in the C-terminal part of the molecule. The current molecular model includes the two molecules of the asymmetric unit, 67 water molecules, and one sulfate ion. The DaFdI overall folding very closely resembles that of ferredoxins of known structure. Comparisons with the single cluster ferredoxins from *Desulfovibrio gigas* and *Bacillus thermoproteolyticus* show that the presence or the absence of a disulfide bridge does not significantly affect the folding of the other half of the molecule, including the characteristic α-helix of the single cluster ferredoxins. Like other ferredoxins or analogs, the [4Fe-4S] iron−sulfur cluster presents, at 2.3 Å resolution, a cubane-like geometry. By contrast, its immediate environment is different as it includes, besides the four cysteic sulfur ligands, the sulfur atom of the free cysteine. This sulfur atom, which is buried within the protein, is in van der Waals contact with one labile sulfur of the cluster and one liganded cysteic sulfur. The association of a [4Fe-4S] cluster with one free cysteic sulfur is similar to that previously found in both X-ray structures of *Azotobacter vinelandii* and *Peptococcus aerogenes* [Stout, C. D. (1989) *J. Mol. Biol. 205*, 545−555; Backes, G., et al. (1991) *J. Am. Chem. Soc. 113*, 2055−2064]. Chemical sequence analysis suggests that this characteristic [4Fe-4S] cluster sulfur environment is widely distributed among ferredoxins.

Sulfate-reducing bacteria have the characteristic and unique ability to couple ATP production to the reduction of sulfate via electron-transfer linked phosphorylation (Peck & Lissolo, 1988). Various electron carriers including *c*-type and *b*-type cytochromes, ferredoxins, flavodoxins, rubredoxins, and menaquinones have been characterized in *Desulfovibrio* species. Most of these molecules are involved in the coupling of substrate oxidation with the terminal reductases (LeGall & Fauque, 1988). Thus, ferredoxins are active in both the phosphoroclastic reaction (Akagi, 1967), sulfite reduction (LeGall & Dragoni, 1966), and, possibly, thiosulfate reduction to sulfide (Hatchikian et al., 1972).

Three distinct ferredoxins, termed ferredoxin I, ferredoxin II, and ferredoxin III (DaFdI, DaFdII, and DaFdIII), have been isolated from the sulfate-reducer *Desulfovibrio africanus*. DaFdI contains a single $[4Fe\text{-}4S]^{2+,1+}$ cluster and five cysteines (Bruschi & Hatchikian, 1982; and this paper). DaFdII contains a spectroscopically similar $[4Fe\text{-}4S]^{2+,1+}$ center and also five cysteines (Hatchikian et al., 1979, 1984; Pieulle, personal communication). DaFdIII, when aerobically isolated, contains two clusters, one $[3Fe\text{-}4S]^{1+,0}$ and one $[4Fe\text{-}4S]^{2+,1+}$ (Armstrong et al., 1989), and seven cysteine residues (Bovier-Lapierre et al., 1987). The redox potentials of ferredoxins I and II are the same (−385 mV; Hatchikian et al., 1984). The redox potentials of ferredoxin III are −140 mV for the $[3Fe\text{-}4S]^{1+,0}$ cluster and −410 mV for $[4Fe\text{-}4S]^{2+,1+}$ cluster. All three ferredoxins show the same efficiency in both phosphoroclastic reactions and H_2-sulfite reductase metabolism (Hatchikian et al., 1979; Hatchikian & Bruschi, 1981).

Sequence comparisons have shown that the three *D. africanus* ferredoxins belong to a large family of low potential bacterial ferredoxins which are characterized by a core of ca. 55−60 residues chelating one or two iron sulfur clusters (dicluster or monocluster type ferredoxins; Fukuyama et al., 1988). The iron sulfur clusters are either [3Fe-4S] or [4Fe-4S] or both [for a review, see Cammack (1992)]. Several X-ray structures of dicluster and monocluster ferredoxins have been determined so far (Adman et al., 1973; Backes et al., 1991; Adman, personal communication; Fukuyama et al., 1988, 1989; Stout, et al., 1988; Stout, 1989; Kissinger et al., 1991; Merritt et al., 1993).

‡ The atomic coordinates have been deposited with the Protein Data Bank under accession number 1FXR.

* Corresponding author. E-mail: frey@llcp.ibs.fr.

§ CEA-CNRS.

|| Present address: Department of Biochemistry, University of Alberta, Edmonton, AB T6G 2H7 Canada.

⊥ Unité de Bioénergétique et Ingéniérie des Protéines.

⊗ Abstract published in *Advance ACS Abstracts,* November 15, 1994.

0006-2960/94/0433-15408$04.50/0

Recent spectroscopic studies (UV absorption, low-temperature magnetic circular dichroism, and NMR) and analyses of highly purified protein samples of *D. africanus* ferredoxin I have revealed that this protein contains one tryptophan and one histidine residue (Davy et al., 1995) which had not been reported in the previously published sequence (Bruschi & Hatchikian, 1982). This confirmed early amino acid analyses and UV spectroscopic studies (Hatchikian et al., 1979). Therefore, we redetermined the chemical sequence of DaFdI in parallel with the determination of its 3D structure by both NMR (Davy et al., 1995) and X-ray methods (this paper).

SEQUENCE DETERMINATION

Materials and Methods

The bacterium *D. africanus* was grown and ferredoxin subsequently isolated in yields of 50 mg of protein/800 g of cells (wet weight) as described previously (Hatchikian et al., 1979).

The amino acid sequence was redetermined using a modified apoprotein preparation (Hong & Rabinowitz, 1967). To minimize the degradation of unstable residues such as tryptophan, we used 10% (v/v) trichloracetic acid at room temperature rather than 3% (v/v) HCl at 80 °C as reported previously (Bruschi & Hatchikian, 1982). The apoprotein preparation (4 mg) was reduced and carboxymethylated according to the method of Crestfield et al. (1963). Amino acid analyses were performed with a Beckman automatic autoanalyser model 6300 (Beckman). Composition of the whole reduced *S*-carboxymethylated protein was obtained by averaging the results (obtained each time from two samples) after 24, 48, and 72 h of hydrolysis in sealed tubes by 6 M tridistilled HCl at 110 °C. Tryptophan content was measured after 22 h hydrolysis at 110 °C in 3 N mercaptoethanesulfonic acid (Penke et al., 1974).

Tryptic peptides were obtained using 2 mg of *S*-carboxymethylated ferredoxin I incubated for 6 h at 37 °C with trypsin (1:15 w/w) in 2 mL of ammonium acetate, pH 8.5. The reaction was stopped by addition of 40 μL of 4-aminophenylmethanesulfonyl fluoride (APMSF)[1] in ammonium acetate solutions (0.4 mg/mL). Cyanogen bromide cleavage was made on 0.3 mg of *S*-carboxymethylated ferredoxin I in 70% TFA (Morrisson et al., 1990). Digestion with carboxypeptidase P was performed at 30 °C on 50 μg of *S*-carboxymethylated protein in 10 mM sodium acetate pH 3.7 according to Yokoyama et al. (1981). The enzyme/substrate ratio was 1:50, and digestions lasted from 10 min to 4 h. The reaction was stopped by addition of 50 μL of acetic acid, and the resulting mixture was directly submitted to the amino acid analyzer.

N-terminal sequence analyses were performed by stepwise Edman degradation using a gas-phase sequencer model 470A (Applied Biosystems). The fragments resulting from enzymatic and chemical cleavages of the *S*-carboxymethylated protein were isolated by reverse-phase HPLC on a C18 10-μm Vidac column (4.6 mm × 250 mm) with a linear gradient from 0 to 90% of acetonitrile/TFA (0.06%) in water/TFA (0.1%). The elution was monitored by absorbance at 228 nm. When necessary, peptides were purified in the same manner but with a flatter gradient.

[1] Abbreviations: APMSF, (4-aminophenyl)methanesulfonyl fluoride; RCM-protein, reduced and carboxymethylated protein; EDTA, ethylenediaminetetracetate sodium salt; HPLC, high-pressure liquid chromatography.

Table 1: Amino Acid Composition of Ferredoxin from *D. africanus* and of Peptides T3 from Tryptic Digestion and CNBr3 from Cyanogen Bromide Cleavage

amino acid	ferredoxin[a]	T3	CNBr3
Cys[b]	5.21 (5)	1.79 (2)	1.55 (2)
Asx	6.24 (6)	3.01 (3)	1.96 (2)
Thr	1.02 (1)	0.97 (1)	0.84 (1)
Ser	1.73 (2)	1.01 (1)	tr[c] (0)
Glx	15.53 (15)	8.61 (9)	3.06 (3)
Pro	3.06 (3)	1.11 (1)	0.93 (1)
Gly	2.19 (2)	1.39 (1)	0.44 (0)
Ala	8.05 (8)	1.98 (2)	tr (0)
Val	6.02 (6)	2.88 (3)	1.01 (1)
Met	1.81 (2)	0.28 (1)	tr (0)
Ile	3.87 (4)	0.94 (1)	0.95 (1)
Leu	tr (0)	tr (0)	tr (0)
Tyr	1.94 (2)	tr (0)	tr (0)
Phe	2.01 (2)	tr (0)	tr (0)
His	0.91 (1)	0.96 (1)	0.93 (1)
Lys	3.07 (3)	tr (0)	tr (0)
Arg	1.06 (1)	tr (0)	tr (0)
Trp[d]	1.00 (1)	ND[e] (1)	ND (1)

[a] The values presented are the average of three analyses. Values in brackets indicate the residues found by sequencing. [b] Measured as carboxymethylcysteine. [c] tr, present only at trace level. [d] Determined by the method of Penke et al. (1974). [e] ND, not determined.

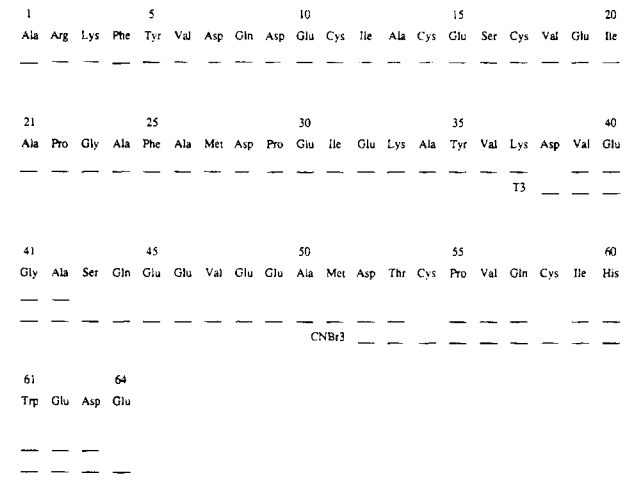

FIGURE 1: Complete amino acid sequence of ferredoxin I of *D. africanus*. The amino-terminal sequence was obtained from *S*-carboxymethylated whole protein. Peptide T3 was obtained from a tryptic digest, and peptide CNBr3 was obtained from cyanogen bromide cleavage. The line (—) below the sequence shows Edman degradation on peptides.

Results

Analysis of the amino acid composition shows that DaFdI contains 64 residues (Table 1) and not 61 as published before (Bruschi & Hatchikian, 1982).

The major portion of DaFdI was sequenced from the intact *S*-carboxymethylated protein. Microsequencing of 4 nmol of protein confirmed that the first 42 residues were the same as those previously reported (Figure 1). Tryptic peptides of ferredoxin were prepared and subsequently separated by reverse-phase high-performance liquid chromatography (HPLC). Sequence determination of about 1 nmol of the peptide T3 (Figure 1) has allowed us to determine the chemical sequence of the protein up to the sixty-third residue including one tryptophan and one histidine residue near the C-terminal end. As an additional check, the *S*-carboxy-

methylated protein was cleaved by cyanogen bromide and the peptide, termed CNBr3, containing histidine, fully sequenced. Both T3 and CNBr3 peptide sequences corroborated their amino acid composition (Table 1). Moreover, digestion of the *S*-carboxymethylated whole protein by carboxypeptidase P released two glutamic acid for one aspartic residue even after three hours incubation.

Therefore, the sequence from Gln^{57} is Gln-Cys-Ile-His-Trp-Glu-Asp-Glu and not Gln-Ser-Ile-Glu-Glu as published by Bruschi and Hatchikian (1982). It is of interest to note that this corrected sequence includes (i) the histidine and tryptophan residues detected by early amino acid analysis and spectroscopic methods and (ii) a fifth cysteine.

X-RAY STRUCTURE DETERMINATION

Crystallization and Characterization. A first crystal form of DaFdI was obtained by the hanging-drop method (Wlodawer & Hodgson, 1975) at room temperature, with 53−65% saturated ammonium sulfate, 0.1 M sodium acetate buffer at pH 5, and 26.6 mg/mL for protein solution. Large crystals (0.3 × 0.3 × 0.2 mm^3) could be grown within 1−3 days. They were characterized by precession photographs as belonging to the cubic space group $P23$ with a rather large cell (a = 126 Å). Furthermore, the mosaicity of these crystals was relatively important (1−1.5°), and the X-ray data did not extend beyond 3.1-Å resolution. Therefore, a new crystal form was sought for.

After numerous trials, brown lath-shaped needle-like crystals were obtained within 1 month at 4 °C and, again, by hanging drop technique. The solutions contained 20 mg/mL protein, 60−66% saturated ammonium sulfate, and 0.1 M sodium acetate buffer at pH 5. Since these crystals frequently grew from rosette-shaped clusters and were often multiple, dioxane at 2% by volume was added to the solutions so that monocrystals could be produced. The crystals are orthorhombic: space group $P2_12_12$ with a = 96.6 Å, b = 58.1 Å, and c = 20.7 Å. They contain two ferredoxin molecules per asymmetric unit. This corresponds to $V_m \approx$ 2.13 $Å^3$/dalton (Mathews, 1968). The diffraction patterns are of good quality with observable reflections to 2.3-Å resolution. Therefore, we used this second crystal form to collect the data and solve the three-dimensionnal structure of the protein.

X-ray Data Collection and Processing. X-ray diffraction data were collected with a fast scanning area sensitive TV detector on a four-circle κ-geometry goniometer (FAST diffractometer, Enraf Nonius) and a rotating anode X-ray generator Enraf Nonius FR571 (Cu Kα radiation λ = 1.5418 Å, 40 kV, 100 mA, with a graphite monochromator). Three data sets were collected from three different crystals, by rotating around the b, c, and a axes, respectively, in order to record simultaneously on the two-dimensional area detector, the intensities corresponding to the Bijvoet mates $[h,\pm k,l]$, $[h,k,\pm l]$, and $[\pm h,k,l]$, respectively. This procedure was used in order to optimize the measurement of the anomalous diffraction signal. This anomalous diffraction signal is due mainly to the iron atoms and to a lesser extent to sulfur atoms.

X-ray data were processed with the program MADNES (Messerschmidt & Pflugrath, 1987; Pflugrath & Messerschmidt, 1989) and the program PROCOR for intensity integration by profile fitting by the method of Kabsch (1988). The three sets of data were merged by the program PROTEIN (version 3.0; Steigemann, 1991) (Table 2). Taking in account only the reflections with $F > 2\sigma(F)$, the resulting set of unique reflections contains 95.1% of the total number of reflections theoretically observable at 2.5-Å resolution, with 70.6% of Bijvoet mates. The R_{merge} corresponding to these three sets of data is 8.6%.

Table 2: Data Collection Statistics

crystal	rotation axis	scan width	observations	2θ	R_{sym}[a]	unique reflections[b]	maximum of resolution (Å)
1	b	60°	3924	15°	5%	1646 (4228)	2.5
2	c	70°	4336	15°	4.4%	2049 (4228)	2.5
3	a	200°	16088	18°	3.8%	4106 (5782)	2.3

[a]

$$R_{sym} = \frac{\sum_{\mathbf{h}}\sum_{N_{\mathbf{h}}}||F(\mathbf{h})| - \langle|F(\mathbf{h})|\rangle|}{\sum_{\mathbf{h}}\sum_{N_{\mathbf{h}}}\langle|F(\mathbf{h})|\rangle}$$

with

$$\langle|F(\mathbf{h})|\rangle = \frac{1}{N_{\mathbf{h}}}\sum_{i=1}^{N_{\mathbf{h}}}|F(\mathbf{h})|$$

where $\Sigma_{\mathbf{h}}$ is the sum over all observed unique reflections and $\Sigma_{N_{\mathbf{h}}}$ the sum over the $N_{\mathbf{h}}$ replicated or symmetry-related observed reflections corresponding to the unique reflection $\mathbf{h}$. [b] Numbers in parentheses represent the number of possible reflections.

Computational Methods. At first, we tried to solve the DaFdI three-dimensional structure by using only the phase information coming from the anomalous diffraction signal measured between Bijvoet mates, following the method developed by Hendrickson et al. (1985). The first step of this method is to determine the position of Fe atoms in the lattice cell. This can be made by calculating and solving an anomalous difference Patterson map with the coefficients ΔF^2 with ΔF given by (Rossman, 1961):

$$\Delta F = F_{obs}(\mathbf{h}) - F_{obs}(\mathbf{h}')$$

where $\mathbf{h}$ is a given reciprocal lattice vector and $\mathbf{h}'$ its Friedel mate $-\mathbf{h}$ or a Bijvoet mate of $\mathbf{h}$ equivalent to $-\mathbf{h}$.

The first striking result shown by this difference Patterson map was a very strong peak at the intersection of the Harker sections Z = 0 and $Y = {}^1/_2$. A similar peak was also found, as the highest peak, in standard Patterson maps calculated with the coefficients F_{obs}^2. It came clear rapidly that these peaks were due to the existence in the crystal of a noncrystallographic 2-fold axis relating the two Fd molecules in the asymmetric unit, this 2-fold axis being parallel to the crystallographic 2-fold axis c. Indeed, rotating a molecule successively around two parallel 2-fold axes is equivalent to translating the molecule on a distance equal to twice the distance between the two axes. From the position of the peak in the Patterson map, by using very simple geometry, it is thus possible to determine the position of the noncrystallographic 2-fold axis in the lattice cell. But as a consequence of the existence of this noncrystallographic 2-fold axis, the interpretation of the anomalous difference Patterson map was difficult. In this case, peaks in the Z = 0 Harker section can be interpreted either as Harker peaks corresponding to each one of the two molecules of the asymmetric unit or as intermolecular cross-peaks between these two molecules. Because of this complexity, no reliable solution of the anomalous difference Patterson map could

be found. The center of gravity of the two Fe-S clusters were located by systematic search, by calculating the agreement factor between the F_{calc}'s calculated with the Fe atoms alone for each tentative cluster position (the position of the second cluster being deduced from the first by the known noncrystallographic 2-fold axis symmetry) and the measured $|\Delta F|$'s. This was carried out at intermediate resolution. The use of the same search technique for finding the orientation of the clusters failed. This is due to the fact that the iron clusters are not highly anisotropic (they show a nearly tetrahedral symmetry), that the resolution of the data is not very high (about 2.5 Å), and that the completeness of the significant anomalous data was poor.

Therefore we undertook to solve the structure of DaFdI by molecular replacement. We used the crystallographic model of the *Desulfovibrio gigas* ferredoxin II at 1.7 Å (DgFdII; Kissinger et al., 1991) since strict sequence homology between DaFdI and DgFdII is 39% and the regions found near the cysteine residues are well conserved in both ferredoxins. We performed the rotation−translation function calculations with the program suite AMoRe (Navaza, 1994). In the early stages of the computation, the DgFdII model has been used without any modification.

X-ray data between 12 and 4 Å were used to determine the orientation and the position of both molecules in the asymmetric unit. The correlation between observed and calculated Patterson functions is 13% for the first rotation solution, and 9.6% for the second. In this case, the first rotation solution determines the orientation of both molecules in the asymmetric unit since the 2-fold noncrystallographic symmetry axis is parallel to the 2-fold *c* axis. The translation function was then used to locate both molecules in the asymmetric unit. The best correlation between observed and calculated structure factors for one molecule was only 23%, but this solution was reasonably contrasted. The location of the second molecule led to a correlation of 52.1%.

Structure Refinement. All the refinement calculations were made with interleaving cycles of refinement with the program X-PLOR (Brünger, 1988) and model building with program O (Jones, 1991) on an Evans and Sutherland ESV20 graphics system.

The first cycle of the refinement consists of three steps: first, a rigid-body refinement was made, considering each of the two molecules as a rigid body. The resulting correlation was 51.2%, and the crystallographic *R* factor was 50.9%. In the second step, the initial DgFdII model was modified so that only the atoms which were identical in both ferredoxins were kept. A new rigid body refinement followed by a refinement of the overall temperature factor *B* and the individual atomic positions was then performed (*R* factor 40.4%). The third step consisted in a refinement of the model by simulated annealing following the X-PLOR tutorial slow cooling protocol [5000 to 300 K, 25 K/0.5 fs; see Brünger and Krukowski (1990)]. During this process we used the 10−2.3-Å resolution X-ray data, and we restrained the two independent molecules in the asymmetric unit to be structurally equivalent (*R* factor 39.9%). A first $(2F_o - F_c)$ electron density map was then calculated. The cluster and its environment appeared well defined for each of the two proteins, but the electron density of many side chains remained too blurred to allow further model building at this stage, particularly in the regions where the sequences of DgFdII and DaFdI are different. This suggested that the bias of the original DgFdII model was still too important.

Therefore, in order to get a less biased estimation of the DaFdI phases, we used the phase information from the anomalous signal following the method of calculation of Hendrickson (1985): (i) we refined the iron atomic positions of the two independent clusters starting from the molecular replacement coordinates, minimizing the quantity

$$R_{cluster} = \frac{\sum||\Delta F| - F_{cl}|}{\sum|\Delta F|}$$

where F_{cl} are the structure factors of the clusters alone. (ii) By combining the structure factors of the clusters calculated with the anomalous scattering amplitude of the Fe atoms, an estimate of the structure factor amplitude of the unknown part of the molecule (based on Wilson's statistics), and the measured anomalous Bijvoet difference ΔF, an evaluation of the phase of the structure factors of the whole molecule can be obtained with its probability distribution function (program A, M. Roth, personal communication). (iii) With these phases, we calculated an electron density map that was then averaged and solvent flattened according to the crystallographic symmetry and with a mask deduced from the molecular replacement model (program AVERG; Vellieux et al., 1993). The necessary rotational and translational matrices relating the two molecules within the asymmetric unit were determined also on the basis of the molecular replacement solution. Finally, a new set of phases was calculated by Fourier inversion of the averaged electron density map and combined with the set of phases obtained by molecular replacement and simulated annealing refinement. The resulting electron density map allowed us to build all the residues located in the vicinity of the [4Fe-4S] cluster and to start identifying some side chains which are different from that of DgFdII. These side chains included particularly Cys^{11} which has a different conformation in DgFdII due to the lack of the fourth iron in the cluster.

The refinement of the DaFdI model proceeded then, again, in a straightforward way through, with about 12 rounds of model building (amino acid substitutions and insertions, adjustment of side chains in electron density map) and refinement cycles (slow cooling followed by energy minimization and individual *B* factor refinement next). At this stage the *R* factor is 24%; however, the electron density corresponding to residues 28−33, the N and C termini, remained poorly defined for both molecules of the asymmetric unit. Interleaving omit-map calculations allowed us to build step by step most residues except for residues 28−33 of the first molecule. This latter segment was eventually built by applying the noncrystallographic symmetry operation to the corresponding segment of the second molecule, and then the two molecules were refined without this noncrystallographic symmetry restraint (*R* factor = 21.5%).

On the resulting $(F_o - F_c)$ map, uninterpreted peaks above 3σ were assigned to oxygen atoms of water molecules, when both their distances to the molecule and the surrounding stereochemistry were acceptable (program WATCONT, D. Housset personal communication). A total of 67 solvent molecules were thus included in the refinement. After this step, we calculated the free *R* value (Brünger, 1992) on the final model. To limit the bias of the model on the test sample, we performed 7 ps of simulated annealing followed by 100 steps of positional refinement. During this last stage, the free *R* value decreased from 0.246 to 0.227, supporting

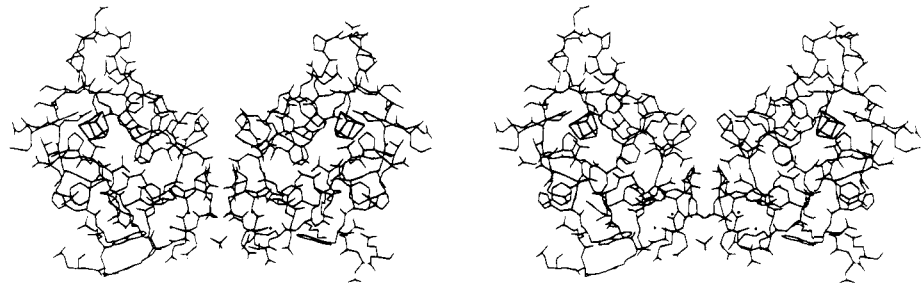

FIGURE 2: Stereoscopic view of the final model. The two ferredoxin molecules of the assymmetric are shown, with their clusters represented by thick lines. The sulfate ion (at the interface) and two buried water molecules (depicted by crosses) are also shown.

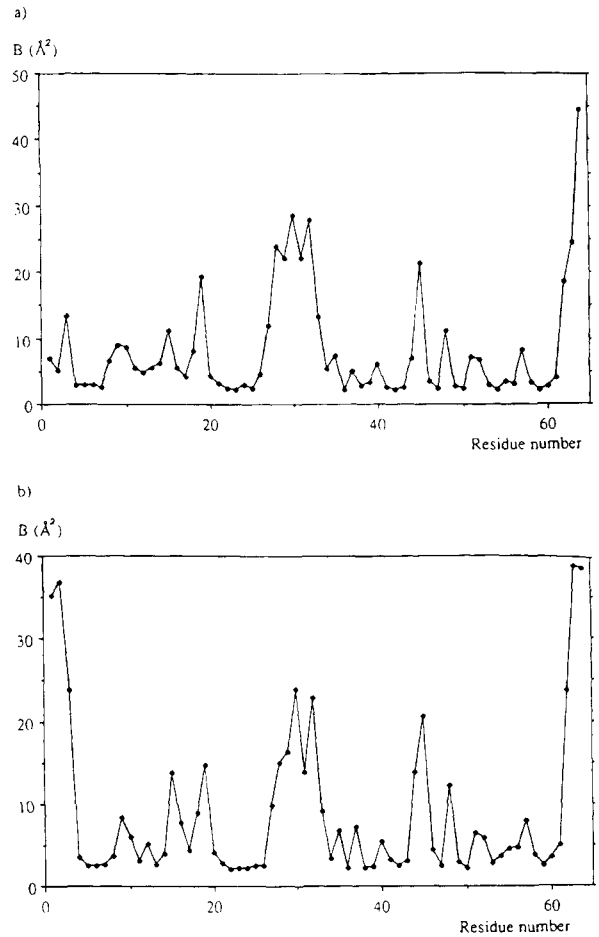

FIGURE 3: Plot of the mean B value versus amino acid residue number: (a) mean temperature factor of the first molecule in the asymmetric unit and (b) mean temperature factors of the second molecule.

the quality of the refined structure. The final R factor is 18.2% in the resolution range 10−2.3 Å for reflections with $F > 2\sigma(F)$ and 18.7% for all reflections. The final model is shown in Figure 2. Relevant refinement statistics are given in Table 3, and the distribution of the mean temperature factors is given in Figure 3.

Results and Discussion

Overall Topology. The electron density of the two molecules of the asymmetric unit (termed molecule I and molecule II) is well-defined (Figure 4) except for (i) the two C-terminal residues, the residues 28−33, and the side chain of Glu[45] in molecules I and II and (ii) the N-terminal residue of molecule II.

A plot of the main-chain dihedral angles for the two molecules (Figure 5) shows that in both molecules most of the residue conformations lie in the energetically allowed regions, except for Asp[63] of the second molecule, the electron density of which is not well defined.

Table 3

Refinement Statistics	
resolution limits (Å)	10−2.3
initial R factor (%)[a]	39.9
final R factor (%)	18.2
no. of reflections used ($F > 2\sigma_F$)	4815
no. of non-hydrogen atoms	1411
overall mean B factor (Å²)	9.6
total no. of solvent molecules	67
Weighted Root-Mean-Square Deviations from Ideality	
bond length (Å)	0.013
bond angle (deg)	2.93
torsion angle (deg)	24.79
improper angle (deg)	1.22

[a] R factor $= (\sum_h |F_{obs} - F_{calc}|)/\sum_h F_{obs}$.

The α-carbon positions in molecules I and II superimpose with a root-mean-square difference of 0.24 Å for amino acid residues 4−62. Their hydrogen bond patterns are also similar (Table 4). This shows that the foldings of the two molecules I and II are equivalent within experimental error. Therefore, from now on we will limit the discussion to molecule I. Several salt bridges can be noted: between Ala[1] N and Glu[40] $O^{\epsilon 2}$, Arg[2] $N^{\eta 2}$ and Asp[63] $O^{\delta 2}$, and Lys[3] N^{ζ} and Glu[62] $O^{\epsilon 2}$ for molecule I. It is also of interest to note that the terminal amide of Arg[2] and the ring of Trp[61] are stacked in molecule I (in molecule II the two first N-terminal residues are disordered).

The secondary structural elements include two α-helices (residues 16−20 and 44−53), two two-stranded sheets [residues 3−6 and residues 59−62 (first sheet); residues 25−28 and residues 33−36 (second sheet)], and five turns (residues 8−10, 22−24, 29−32, 39−40, and 55−56) (Figure 6a). This seems to be another case where the absence of the second cluster is correlated with the presence of an α-helix (44−53), as mentioned by Fukuyama et al. (1988).

The [4Fe-4S] cluster is covalently bound to the four cysteines 11, 14, 17, and 54 through Fe−S^{γ} bonds. It has also to be pointed out that Cys[58] S^{γ} atom is in van der Waals contact with one S atom of the [4Fe-4S] cluster (Figure 6b). The cluster geometry is, within experimental error, very similar to those found in previously determined three-dimensional X-ray structures of ferredoxins, e.g., *Peptococcus aerogenes* (PaFd), *Azotobacter vinelandii* (AvFd), and *Bacillus thermoproteolyticus* (BtFd) (Adman et al., 1973; Backes et al., 1991; Stout, 1989; Fukuyama et al., 1989). In particular, three of the four cysteic S^{γ} atoms bound to the cluster and three of the four inorganic sulfur atoms from the cluster are involved in NH···S bonds with main-chain amide

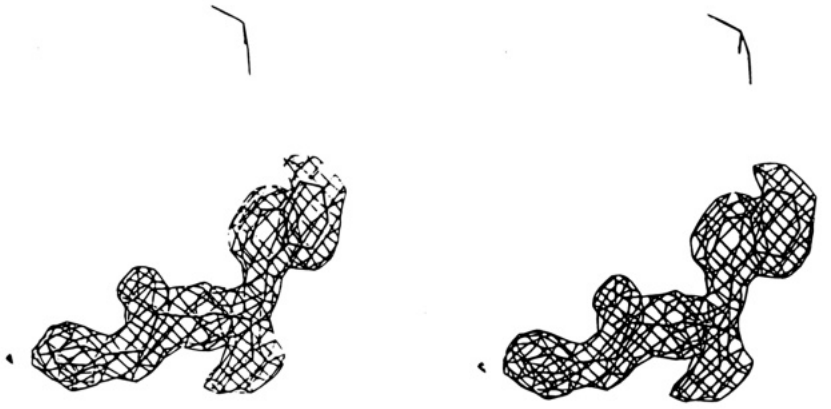

FIGURE 4: Final ($2F_o - F_c$) map of *D. africanus* FdI in stereo. A well-defined region of electron density showing residues His^{60} and Trp^{61}. The map is contoured at the 1σ level, where σ is the rms deviation of the density in the map.

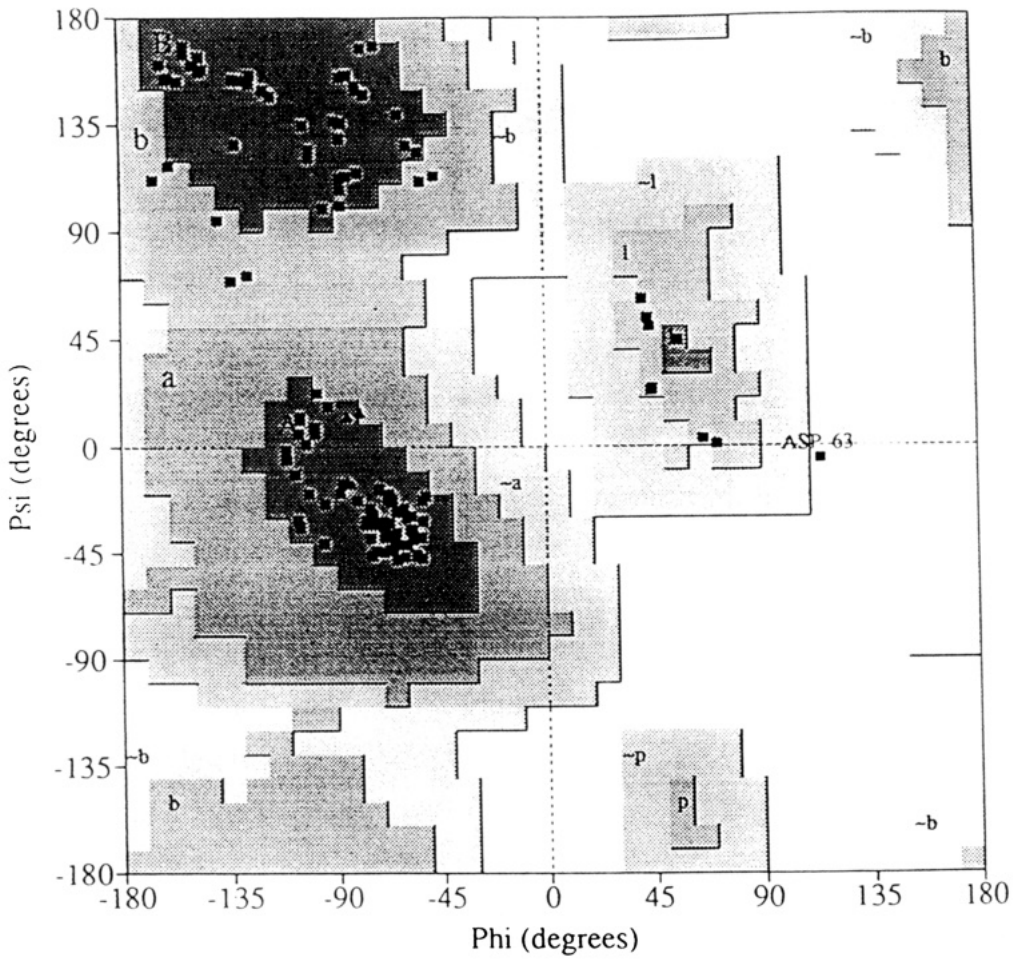

FIGURE 5: Ramachandran plots of all main dihedral angles for the first molecule (a) and the second molecule (b) in the asymmetric unit. The energetically allowed regions for nonglycine residues are indicated in grey (Ramachandran et al., 1963).

nitrogen atoms of the protein (Table 5) (Carter et al., 1974; Adman et al., 1975; Kissinger et al., 1991).

Crystal Packing. The DaFdI molecules form layers parallel to the (*a*,*b*) plane which are close-packed in the *c* direction: their diameters in the *c* direction are nearly equal to *c*. The two molecules within the asymmetric unit are tightly linked by seven intermolecular hydrogen bonds involving residues 38, 40−43, and 46. Interestingly, $O^{\delta 1}$ of Asp^{38} (mol I) is at hydrogen bond distance of $O^{\epsilon 1}$ of Glu^{46} (mol II), and, reciprocally, $O^{\delta 1}$ of Asp^{38} (mol II) is at hydrogen bond distance of $O^{\epsilon 2}$ of Glu^{46} (mol I), indicating that one of the carboxyl groups should be protonated. This assumption seems compatible with the pH of the crystals. By contrast, at neutral pH this type of interaction is likely to be unfavorable. Along these same lines, ultracentrifugation experiments have shown that DaFdI is monomeric. Therefore, it seems that the dimer which has been observed in the crystal is not biologically relevant. Otherwise there are no large contact areas with other symmetry-related molecules.

Structural Comparisons with Bacterial Ferredoxins: Overall Comparisons with Monocluster Ferredoxins. DaFdI is 39% homologous with DgFdII and 31% with BtFd with respect to the amino acid sequence. The X-ray model of DaFdI has been compared to the model structures of DgFdII (Kissinger et al., 1991) and BtFd (Fukuyama et al., 1989) deposited at the Brookhaven Protein Data Bank (Bernstein et al., 1977; Abola et al., 1987). We superimposed the

Table 4

		molecule I		molecule II	
D[a]	A[b]	distance (Å)	angle (deg)[c]	distance (Å)	angle (deg)[c]
(a) Hydrogen Bonds Involving Main-Chain Atoms					
N 5	O 60	3.07	146.7	3.12	151.6
N 7	O 58	2.74	139.0	2.75	154.2
N 10	O 7	3.3	148.3	3.12	158.9
N 11	O 8	3.35	141.0	3.36	147.1
N 13	O 11	3.45	135.5		
N 18	O 15	3.6	138.7	3.16	137.0
N 19	O 15	3.07	163.5	3.04	155.5
N 20	O 16	2.88	158.6	2.86	163.1
N 21	O 17	2.85	150.8	2.96	162.7
N 24	O 21	3.1	149.1	3.05	151.8
N 25	O 21	2.96	154.1	2.98	154.8
N 26	O 35	3.2	158.9	3.15	160.5
N 28	O 33	2.85	177.8	2.86	172.8
N 31	O 28	3.09	139.1	3.27	140.4
N 32	O 28	2.89	143.2		
N 35	O 26	2.94	155.1	3.06	153.0
N 37	O 24	2.78	138.2	2.86	140.1
N 38	O 24	2.78	160.9	3.46	155.2
N 41	O 38	3.02	157.3	2.96	151.9
N 47	O 43	3.03	158.6	2.98	164.0
N 48	O 44	3.04	170.6	2.98	160.7
N 49	O 45	2.98	156.7	3.02	155.4
N 50	O 46	3.15	156.2	3.14	161.6
N 51	O 47	2.87	163.1	2.89	168.2
N 52	O 48	2.8	154.8	2.84	167.2
N 53	O 49	2.98	155.5	2.96	155.8
N 54	O 50	3.02	150.1	2.97	138.3
N 57	O 54	2.93	162.4	2.97	160.7
N 60	O 5	3.0	162.1	2.99	155.7
N 62	O 3	2.84	156.3	3.06	147.7
(b) Hydrogen Bonds Involving Side-Chain Atoms					
Arg $N^{\epsilon 2}$ 2	Asp $O^{\delta 1}$ 63	2.94	161.1		
Gln $N^{\epsilon 2}$ 8	Ala O 34	2.78	156.4	2.91	167.0
Asp N 9	Asp $O^{\delta 1}$ 7	3.40	129.1		
Asp N 9	Asp $O^{\delta 2}$ 7			3.45	132.2
Glu N 30	Asp $O^{\delta 1}$ 28	3.30	152.1	3.39	133.1
Ile N 31	Asp $O^{\delta 1}$ 28	3.47	137.0		
Lys N^{ζ} 33	Gln O 8	3.02	152.3	2.83	153.0
Glu N 40	Asp $O^{\delta 2}$ 38	3.21	151.7	3.14	155.4
Glu N 46	Ser O^{γ} 43	3.28	158.5	3.14	179.4
Gln $N^{\epsilon 2}$ 57	Met O 51	2.92	139.2		
Gln $N^{\epsilon 2}$ 57	Cys O 54			3.14	152.6

[a] D, donor. [b] A, acceptor. [c] Angle (A, H, D).

Table 5

A[a]	D[b]	molecule I distance (Å)	molecule II distance (Å)
(a) Hydrogen Bonds Type NH···S_{γ}			
S^{γ} 11	N 13	3.55	3.35
S^{γ} 11	N 34	3.44	3.52
S^{γ} 14	N 15	3.37	3.42
S^{γ} 14	N 16	3.57	3.59
S^{γ} 17	N 18	3.44	3.49
S^{γ} 54	N 57	3.61	3.69
S^{γ} 54	N 58	3.63	3.56
(b) Hydrogen Bonds Type NH···S*			
S* 1	N 14	3.62	3.77
S* 1	N 15	3.20	3.29
S* 3	N 12	3.33	3.38
S* 4	N 17	3.69	3.43

[a] A, hydrogen acceptor. [b] D, hydrogen donor.

α-carbon positions of the three ferredoxins DgFdII, BtFd and DaFdI with the program ALIGN (Satow et al., 1986) (Table 7). It appeared that (i) the percentage of residues, the α-carbon of which are distant by less than 1.5 Å, is 77% between DaFdI and DgFdII and 81% between DaFdI and BtFd, and (ii) the cluster environments, the α-helices, and β-sheets are highly conserved. The major differences concern two important insertions in BtFd and, in DgFdII, a disulfide bridge between cysteines 18 and 42 opposite to the unique cluster. Although that disulfide bridge probably plays a role in the protein structure stabilization, its presence or absence does not significantly affect the overall folding. It is also of interest to note that the clusters of BtFd, DgFdI, and DaFdI are excluded from contact with solvent by Tyr^{27}, Met^{24}, and Met^{27}, respectively. This particularly accounts for the relatively high stability of the DaFdI cluster which has been previously observed by spectroscopic studies (Hatchikian et al., 1984).

Table 6: Chelation of the Clusters

		molecule I		molecule II	
		distance (Å)	angle (deg) (FE, S^{γ}, C^{β})	distance (Å)	angle (deg) (FE, S^{γ}, C^{β})
FE1	S^{γ} Cys^{11}	2.31	117	2.14	116
FE2	S^{γ} Cys^{17}	2.22	114	2.00	119
FE3	S^{γ} Cys^{14}	2.01	135	2.13	125
FE4	S^{γ} Cys^{54}	2.14	120	2.19	118

The Additional Fifth Cysteine. As mentioned above, four of the five cysteine residues (11, 14, 17, and 54) in DaFdI chelate the cluster to the protein (Table 6). The remaining "fifth" Cys^{58}, which is fully buried within the protein, is also involved in interaction with the cluster and its immediate environment since $Cys^{58}S^{\gamma}$ is in van der Waals contact with one inorganic sulfur (S; 3.35 Å) and one of the chelating cysteine sulfurs (Cys^{54} S^{γ}; 3.55 Å). This remarkable geometry has also been observed around the [4Fe-4S] cluster of *Azotobacter vinelandii* ferredoxin [X-ray model at 1.9-Å resolution (Stout, 1989)] and the "second" [4Fe-4S] cluster of *P. aerogenes* ferredoxin [X-ray model at 2-Å resolution (Backes et al., 1991; E. T. Adman, personal communication]. This led us to superimpose the iron atoms of DaFdI and AvFd [4Fe-4S] clusters and the "second" (in terms of sequence) liganded [4Fe-4S] cluster of PaFd (Figure 7) and to observe that the cluster cysteic environment, including the "fifth" cysteine, is nearly identical in the three ferredoxins. Furthermore, superposition of the main chain atom positions of the three ferredoxins PaFd, AvFd, and DaFdI with the program ALIGN (Satow et al., 1986) (Table 8) showed that (i) the number of residues, the main chain atoms of which are distant by less than 1.5 Å, is ca. 30, and (ii) the structurally most conserved regions includes the "additional" cysteine.

Crystallographic analyses (Martin et al., 1989; Soman et al., 1991), reduction potential, and reactivity studies of two mutants of *A. vinelandii* ferredoxin (C20A and C24A; Iismaa et al., 1991) suggested that a direct interaction between the "fifth" cysteine (Cys^{24}) and the cluster may account for the difference in potential between the wild-type protein (−647 mV) and the C24A mutant (−600 mV). These same studies suggested that the irreversible oxidation of the [4Fe-4S] cluster by $Fe(CN)_6^{3-}$ requires, in a first step, the formation of a cysteinyl disulfide radical (Cys-S-S•) involving Cys^{24}. However, this point is not in accordance with previous spectroscopic studies which did not reveal any radical in DaFdI after ferricyanide treatment (Hatchikian et al., 1984). It is also of interest to note that in the *A. vinelandii* mutant C20A Cys^{24} "replaces" Cys^{20} as a cluster ligand following a rearrangement of the protein structure (Martin et al., 1991). In any event, it can be expected that the presence of an

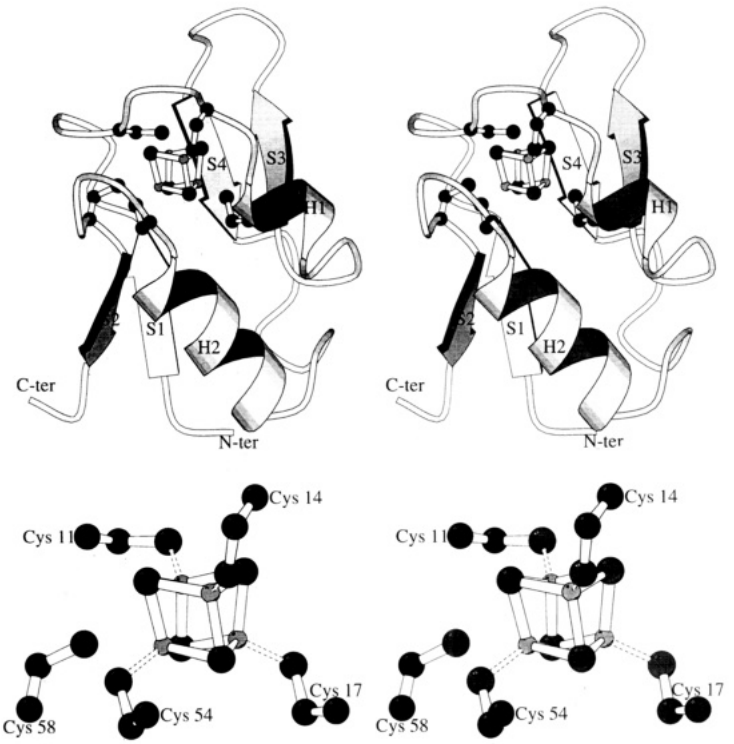

FIGURE 6: (a, top) Schematic drawing of the ferredoxin molecule: strands of β-sheet are shown as gray arrows; α-helices are shown as gray ribbons. The [4Fe-4S] cluster and the five cysteines are represented as ball and stick: dark gray for carbons, medium gray for sulfur, and light gray small balls for iron. This figure was generated by using the program MOLSCRIPT (Kraulis, 1991). (b, bottom) Close-up of the cluster, in the same orientation. It shows the four cysteine residues which chelate the cluster (11, 14, 17, and 54) and the additional "fifth" cysteine residue (58).

Table 7: Structural Alignment of DgFdII and BtFd on DaFdI Model[a]

					5					10					15					20					25				
DafdI	a	R	K	F	Y	V	D	Q	D	E	C	I	A	C	E	S	C	V	E	I	A	P	G	A	F	A	M	D	P
DgFdII			p	I	E	V	N	-	D	D	C	M	A	C	E	A	C	V	E	I	C	P	D	V	F	E	M	N	E
BtFd	p	K	Y	T	I	V	D	K	E	T	C	I	A	C	G	A	C	G	A	A	A	P	D	I	Y	D	Y	D	E

	30					35					40					45					50					55			
DafdI	e	i	E	K	A	Y	V	K	D	v	e	g	a	S	Q	E	E	V	E	E	A	M	D	T	C	P	V	Q	C
DgFdII	e	g	D	K	A	V	V	I	N	p	d	s	d	L	-	D	C	V	E	E	A	I	D	S	C	P	A	E	A
BtFd	-	d	g	I	A	Y	V	T	L	&	-	-	-	L	I	D	D	M	M	D	A	F	E	G	C	P	T	D	S

	60					64
DafdI	I	H	W	E	D	E
DgFdII	I	V	R	S		
BtFd	I	K	V	#		

[a] Superimposed residues (closer than 1.5 Å) appear as uppercase letters. Main-chain atoms were superimposed with the program Align (Satow et al., 1986). The rms difference is 0.73 Å for DgFdII (203 pairs) and 0.69 Å for BtFd (204 pairs). Symbols: (&) D D N Q G I V E V P D I; (#) A D E P F D G D P N K F E.

additional sulfur in the cluster immediate environment plays a role in electron transfer between the cluster and the protein surface.

Moreover, sequence alignments of bacterial ferredoxins had already shown the presence of an invariant cysteine, four residues further than a cysteic iron ligand, in some families of ferredoxins (Otaka & Ooi, 1987; Iismaa et al., 1991; Matsubara & Saeki, 1992). Following our present study we can expect that the sulfur atom of these "additional" cysteines is also in van der Waals contact with a cluster. For example, in the ferredoxin II from *Desulfovibrio vulgaris* Miyazaki (DvFdII; 63 residues, one [4Fe-4S] cluster, seven cysteines; Okawara et al., 1988), four cysteic sulfur atoms probably ligand the [4Fe-4S] cluster (Cys^{11}, Cys^{14}, Cys^{17}, and Cys^{53}),

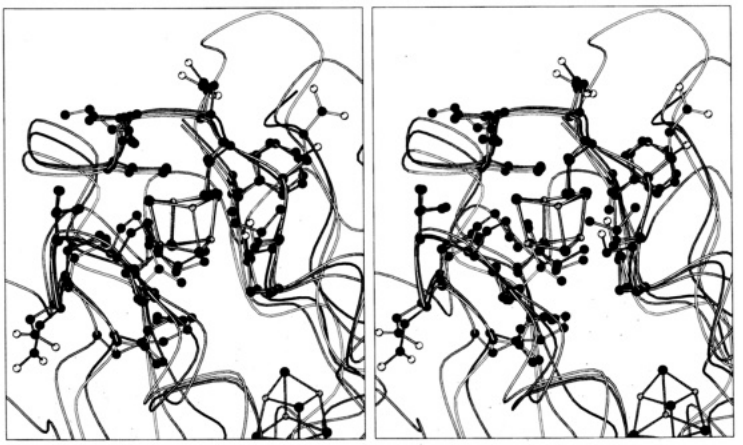

FIGURE 7: Superposition of the [4Fe-4S] cluster and their environments: *D. africanus* FdI, *P. aerogenes* ("second" cluster), and *A. vinelandii* ferredoxins.

Table 8: Structural Alignment of AvFd and PaFd on DaFdI Model[a]

DafdI	A	R	K	F	5 Y	V	D	Q	D	10 E	C	I	A	C	15 E	S	C	V	E	20 I	A	P	G	A	25 F	A	M	D	P
AvFd				L	33 V	I	H	P	D	38 E	C	I	D	C	43 A	L	C							A	54 I	F	S		
PaFd					30 A	I	D	A	D	35 S	C	I	D	C	40 G	S	C	A	S	45 V						52 N	P		

DafdI	30 E	I	E	K	A	35 Y	V	K	D	V	40 E	G	A	S	Q	45 E	E	V	E	E	50 A	M	D	T	C	55 P	V	Q	C
AvFd				A	F	3 V	V															17 V		V	C	21 P	V	D	C
PaFd				A	Y	3 V	I															K	P	E	C	19 P	V	N	C

DafdI	I	60 H	W	E	D	64 E	
AvFd							
PaFd	I	24 Q					

[a] For AvFd and PaFd, only superimposed residues (all main-chain atoms closer than 1.5 Å) are shown, with their respective numbering. Main-chain atoms were superimposed with the program Align (Satow et al., 1986). The rms difference is 0.60 Å for AvFd (116 pairs) and 0.61 Å for PaFd (124 pairs).

two form a disulfide bridge (Cys^{21} and Cys^{45}), and one is in van der Waals contact with the cluster (Cys^{57}). Along these same lines, in the ferredoxin (FdIII) from *Rhodobacter capsulatus* (100 residues, two [4Fe-4S] clusters, nine cysteines; Jouanneau et al., 1993) eight of the nine cysteic sulfur atoms are probably liganding the two [4Fe-4S] clusters of the protein (Cys^{25}, Cys^{28}, Cys^{31}, and Cys^{88} for the "first" cluster; Cys^{79}, Cys^{82}, Cys^{85}, and Cys^{35} for the "second"), and the "ninth" cysteic sulfur (Cys^{93}) could be in van der Waals contact with the "first" cluster. It is also of interest to note that, the *D. vulgaris* Miyazaki contains, like DaFdI, a tryptophan (Trp^{60}) close to the C-terminal end (Glu^{63}).

Comparisons of several X-ray structures had led to the classification of bacterial ferredoxins according to their cluster structure ([4Fe-4S] or [3Fe-4S]) and content (mono or di cluster ferredoxins) and the presence or the absence of a disulfide bridge (Fukuyama et al., 1988). Further structural and sequence analyses lead us to propose a third type of cluster ([4Fe-4S] only, so far) characterized by a van der Waals contact with a buried free cysteine sulfur. Recent ^1H NMR and Mössbauer studies have suggested that the redox activity of the [3Fe-4S] cluster of *D. gigas* ferredoxin II could be associated with a thiol/disulfide formation between the two cysteines which are not liganded to the cluster (Macedo et al., 1994). In our case, similar biophysical studies are greatly awaited to determine if the "additional" cysteine is functionally relevant or merely structural.

ACKNOWLEDGMENT

We are indebted to Prof. Andrew Thompson and his colleagues for stimulating discussions and to Dr. Elinor Adman for the communication of the recently refined models of the *P. aerogenes* and *D. gigas* ferredoxins. We acknowledge Nicole Forget for the purification of the tryptic peptides

and Nicole Zylber for performing amino acid analysis. We thank Dr. Claudine Cohen-Addad and Dr. Otto Dideberg for the use of their FAST diffractometer.

REFERENCES

Abola, E. E., Bernstein, F. C., Bryant, S. H., Koetzle, T. F., & Weng, J. (1987) *Information Content Software Systems, Scientific Applications* (Allen, F. H., Bergerhoff, G., & Sievers, R., Eds.) pp 107−132, Data Commission of the International Union of Crystallography, Bonn/Cambridge/Chester.

Adman, E. T., Sieker, L. C., & Jensen, L. H. (1973) *J. Biol. Chem. 248*, 3987−3996.

Adman, E., Watenpaugh, K. D., & Jensen, L. H. (1975) *Proc. Natl. Acad. Sci. U.S.A. 72*, 4854−4858.

Akagi, J. M. (1967) *J. Biol. Chem. 242*, 2478−2483.

Armstrong, F. A., George, S. J., Cammack, R., Hatchikian, E. C., & Thomson, A. J. (1989) *Biochem. J. 264*, 265−273.

Backes, G., Mino, Y., Loehr, T. M., Meyer, T. E., Cusanovich, M. A., Sweeney, W. V., Adman, E. T., & Sanders-Loehr, J. (1991) *J. Am. Chem. Soc. 113*, 2055−2064.

Bernstein, F. C., Koetzle, T. F., Williams, G. J. B., Meyer, E. F., Jr., Brice, M. D., Rodgers, J. R., Kennard, O., Shomanouchi, T., & Tasumi, M. (1977) *J. Mol. Biol. 112*, 535−542.

Bovier-Lapierre, G., Bruschi, M., Bonicel, J., & Hatchikian, E. C. (1987) *Biochim. Biophys. Acta 913*, 20−26.

Brünger, A. T. (1988) in *Crystallographic Computing 4: Techniques and Technologies* (Isaac, N. W., & Taylor, M. R., Eds.) pp 126−140, Clarendon Press, Oxford.

Brünger, A. T. (1992) *Nature 355*, 472−474.

Brünger, A. T., & Krukowski, A. (1990) *Acta Crystallogr. A46*, 585−593.

Bruschi, M., & Hatchikian, E. C. (1982) *Biochimie 64*, 503−507.

Cammack, R. (1992) *Advances in Inorganic Chemistry. Iron−Sulfur Proteins*, Academic Press, New York.

Carter, C. W., Jr., Kraut, J., Freer, S. T., & Alden, R. A. (1974) *J. Biol. Chem. 249*, 6339−6346.

Crestfield, A. M., Moore, S., & Stein, W. H. (1963) *J. Biol. Chem. 239*, 622−627.

Davy, S. L., Breton, J., Osborne, M. J., Thomson, A. J., Thurgood, A. P., Lian, L.-Y., Moore, G. R., Thurgood, A. P., & Hatchikian, C. (1995) *Biochim. Biophys. Acta* (in press).

Fukuyama, K., Nagahara, Y., Tsukihara, T., Katsube, Y., Hase, T., & Matsubara, H. (1988) *J. Mol. Biol. 199*, 183−193.

Fukuyama, K., Matsubara, H., Tsukihara, T., & Katsube, Y. (1989) *J. Mol. Biol. 210*, 383−398.

Hatchikian, E. C., & Bruschi, M. (1981) *Biochim. Biophys. Acta 634*, 41−51.

Hatchikian, E. C., LeGall, J., Bruschi, M., & Dubourdieu, M. (1972) *Biochim. Biophys. Acta 258*, 701−708.

Hatchikian, E. C., Jones, H. E., & Bruschi, M. (1979) *Biochim. Biophys. Acta 548*, 471−483.

Hatchikian, E. C., Cammack, R., Patil, D. S., Robinson, A. E., Richards, A. J. M., George, S. J., & Thomson, A. J. (1984) *Biochim. Biophys. Acta 784*, 40−47.

Hendrickson, W. A., Smith, J. L., & Sheriff, S. (1985) *Methods Enzymol. 115*, 41−55.

Hong, J.-S., & Rabinowitz, J. C. (1967) *Biochem. Biophys. Res. Commun. 29*, 246−252.

Iismaa, S. E., Vazquez, A. E., Jensen, G. M., Stephens, Ph. J., Butt, J. N., Armstrong, F., & Burgess, B. K. (1991) *J. Biol. Chem. 266*, 21563−21571.

Jones, T. A., Zou, J.-Y., Cowan, S. W., & Kjeldgaard, M. (1991) *Acta Crystallogr. A47*, 110−119.

Jouanneau, Y., Meyer, C., Gaillard, J., Forest, E., & Gagnon, J. (1993) *J. Biol. Chem. 268*, 10636−10644.

Kabsch, W. (1988) *J. Appl. Crystallogr. 21*, 916−924.

Kraulis, P. J. (1991) *J. Appl. Crystallogr. 24*, 946−950.

Kissinger, C. R., Sieker, L. C., Adman, E. T., & Jensen, L. H. (1991) *J. Mol. Biol. 219*, 693−715.

LeGall, J., & Dragoni, N. (1966) *Biochem. Biophys. Res. Commun. 23*, 145−149.

LeGall, J., & Fauque, G. (1988) in *Biology of Anaerobic Microorganisms* (Zehnder, A. J. B., Ed.) pp 587−639, J. Wiley & Sons, Inc., New York.

Macedo, A. L., Moura, I., Surerus, K. K., Papaefthymiou, V., Liu, M.-Y., LeGall, J., Münck, E., & Moura, J. J. J. (1994) *J. Biol. Chem. 269*, 8052−8058.

Martin, A. E., Burgess, B. K., Stout, C. D., Cash, V. L., Dean, D. R., Jensen, G. M., & Stephens, P. J. (1990) *Proc. Natl. Acad. Sci. U.S.A. 87*, 598−602.

Matthews, B. W. (1968) *J. Mol. Biol. 33*, 491−497.

Matsubara, H., & Saeki, K. (1992) *Adv. Inorg. Chem. 38*, 223−280.

Merritt, E. A., Stout, G. H., Turley, S., Sieker, L. C., Jensen, L. H., & Orme-Johnson, W. H. (1993) *Acta Crystallogr. D49*, 272−281.

Messerschmidt, A., & Pflugrath, J. W. (1987) *J. Appl. Crystallogr. 20*, 306−315.

Morrisson, J. R., Fidge, N. H., & Grego, B. (1990) *Anal. Biochem. 186*, 145−152.

Navaza, J. (1994) *Acta Crystallogr. A50*, 157−163, and references therein.

Okawara, N., Ogata, M., Yagi, T., Wakabayashi, S., & Matsubara, H. (1988) *Biochimie 70*, 1815−1820.

Otaka, E., & Ooi, T. (1987) *J. Mol. Evol. 26*, 257−267.

Peck, H. D., Jr., & Lissolo, T. (1988) in *The Nitrogen and Sulphur Cycles* (Cole, J. A., & Ferguson, S. J., Eds.) pp 99−132, Cambridge University Press, Cambridge.

Penke, B., Ferenczy, R., & Kovacs, J. (1974) *Anal. Biochem. 60*, 45−50.

Pflugrath, J. W., & Messerschmidt, A. (1989) MADNES: Munich Area Detector NE System, User's Guide, ENRAF-NONIUS B. V., P.O. Box 483, 2600AL Delft, The Netherlands.

Rossmann, M. G. (1961) *Acta Crystallogr. 14*, 383−388.

Satow, Y., Cohen, G. H., Padlan, E. A., & Davies, D. R. (1986) *J. Mol. Biol. 190*, 593−604.

Soman, J., Iismaa, S., & Stout, C. D. (1991) *J. Biol. Chem. 266*, 21558−21562.

Steigemann, W. (1991) in *Crystallographic Computing 5: from Chemistry to Biology* (Moras, D., Podjarny, A. D., & Thierry, J. C., Eds.) pp 115−125, International Union of Crystallography, Oxford University Press, Oxford.

Stout, C. D. (1989) *J. Mol. Biol. 205*, 545−555.

Stout, G. H., Turley, S., Sieker, L. C., & Jensen, L. H. (1988) *Proc. Natl. Acad. Sci. U.S.A. 85*, 1020−1022.

Vellieux, F. M. D., Hajdu, J., Verlinde, C. L. M. J., Groendijk, H., Read, R. J., Greenhough, T. J., Campbell, J. W., Kalk, K. H., Littlechild, J. A., Watson, H. C., & Hol, W. G. J. (1993) *Proc. Natl. Acad. Sci. U.S.A. 90*, 2355−2359.

Wlodawer, A., & Hodgson, K. O. (1975) *Proc. Natl. Acad. Sci. U.S.A. 72*, 398−399.

Yokoyama, S., Miyabe, T., Oobayashi, A., Tanabe, O., & Ichishina, E. (1981) *Agr. Biol. Chem. 45*, 311−314.